JOURNAL OF MATERIALS SCIENCE: MATERIALS IN MEDICINE 10 (1999) 319–327

The failure of amalgam dental restorations due to cyclic fatigue crack growth

D. AROLA*, M. P. HUANG, M. B. SULTAN
Department of Mechanical Engineering, University of Maryland Baltimore County, 1000 Hilltop Circle, Baltimore MD 21250, USA
E-mail: darola@engr.umbc.edu

In this study a restored mandibular molar with different Class II amalgam preparations was examined to analyze the potential for restoration failure attributed to cyclic fatigue crack growth. A finite element analysis was used to determine the stress distribution along the cavo-surface margin which results from occlusal loading of each restoration. The cyclic crack growth rate of sub-surface flaws located along the dentinal cavo-surface margin were determined utilizing the Paris law. Based on similarities in material properties and lack of fatigue property data for dental biomaterials, the cyclic fatigue crack growth parameters for engineering ceramics were used to approximate the crack growth behavior. It was found that flaws located within the dentine along the buccal and lingual margins can significantly reduce the fatigue life of restored teeth. Sub-surface cracks as short as 25 μm were found capable of promoting tooth fracture well within 25 years from the time of restoration. Furthermore, cracks longer than 100 μm reduced the fatigue life to less than 5 years. Consequently, sub-surface cracks introduced during cavity preparation with conventional dental burrs may serve as a principal source for premature restoration failure.

1. Introduction

It is generally accepted among dentists that a significant portion of their clinical activities are occupied by the replacement of existing restorations. Moore and Stewart [1] estimated that the average dental practitioner allocates almost 40% of their time repairing defective restorations. Indeed, Goldberg *et al*. [2] and White *et al*. [3] independently reported that nearly one-third of all restorations are defective and eventually require repair or complete replacement. More than 50% of these failures are attributed to either a missing or partially missing restoration with evidence of tooth fracture or cracking [3]. Hence, the failure of dental restorations is a significant problem that requires further study.

Based on a number of contributing factors, the primary cause for restoration failures has not been clearly distinguished. Cavity design, cavo-surface margin adhesion, and the methods of cavity preparation (instruments, techniques, etc.) could all contribute to restoration success. Lambert [4] suggested that the likelihood of tooth fracture increases with amalgam size. Indeed, Vale [5] showed that premolar teeth with relatively small restorations are stronger than those with large ones. However, Re and Norling [6] found that the static axial load required to fracture molars with amalgam restorations increased with cavity preparation and size. Therefore, restoration failures may be only partially attributed to cavity design.

Various surface conditioners, primers, and methods of curing have been developed to maximize amalgam retention and diminish restoration failure [7]. Interestingly, Tam and Pilliar [8] suggested that cavo-surface margin adhesion should be examined using fracture mechanics because of a comparatively low adhesive fracture toughness and the presence of interfacial microscopic flaws. Although a refreshing approach, flaws are much more likely present in the tooth resulting from cavity preparation. Indeed, Watson [9, 10] documented the development of sub-surface cracks ahead of the burr when cutting from the buccal surface towards the dentinoenamel junction (DEJ). Watson [11, 12] consequently reasoned that residual sub-surface cracking produces a weak bonding surface. The extent of sub-surface damage which resulted from clinical tooth preparation with abrasive diamond burrs was recently quantified by Xu *et al*. [13]. Sub-surface cracks were found in the prepared enamel that extended to depths of 80 ± 34 μm. Therefore, crack propagation within the enamel or dentine during mastication could be a principal source of restoration failure.

The purpose of this investigation was to examine the potential for restoration failures originating from sub-surface flaws introduced during cavity preparation. A semi-empirical model was used to predict the life of restored mandibular molars with standard Class II amalgam preparations resulting from cyclic fatigue

*To whom all correspondence should be addressed.

crack growth. Based on this investigation, the influence of various oral factors on the integrity of restored teeth are examined, and the implications to future dental practices are discussed.

2. Method of approach

Reports from experimental observations by Watson [9–12] and Xu *et al.* [13] have distinguished that microscopic flaws are frequently introduced to the tooth during cavity preparation. Assuming that the flaw extends below the cavo-surface margin as a crack with negligible root radius, then linear elastic fracture mechanics (LEFM) is an appropriate method for analysis. However, the cyclic stress distribution resulting from mastication undoubtedly promotes fatigue crack propagation.

2.1. Analysis of fatigue crack growth under cyclic loads

If a sub-surface crack is initiated during cavity preparation, then the restoration fatigue life is exhausted entirely through cyclic crack propagation. The incremental fatigue crack growth rate may be determined using the Paris law [14] according to

$$\frac{da}{dN} = C(\Delta K)^m \tag{1}$$

where (da/dN) is the cyclic crack growth rate and a and N are the incremental crack length and number of fatigue cycles, respectively. The Paris law parameters C and m are empirical constants which are dependent on material properties; they are often available from the literature or may be obtained from an experimental analysis. The stress intensity range ΔK in Equation 1 is expressed in terms of the stress state and crack length according to

$$\Delta K = F\Delta\sigma(\pi a)^{1/2} \tag{2}$$

where $\Delta\sigma$ is the stress range $(\sigma_{max} - \sigma_{min})$ and F is a geometry factor which accounts for geometry and boundary conditions. The number of cycles to failure (N_f) or restoration ''fatigue life'' can be found by integrating Equation 1 over the limits of integration from the initial a_i to the final crack length a_f. Rewriting Equation 1 for the fatigue life then gives

$$N_f = \int_{a_i}^{a_f} \frac{da}{C(\Delta K)^m} \tag{3}$$

Since the geometry factor F is also a function of the flaw length and changes with crack growth, the integral expression in Equation 3 cannot be solved in closed form. However, it is often assumed that the geometry factor does not change appreciably with crack growth from that evaluated at the initial crack length; this becomes most appropriate for brittle materials which are extremely flaw sensitive. The final crack length a_f in Equation 3 is the critical flaw length which promotes failure at the maximum applied stress. According to LEFM, a_f may be conveniently found from

$$a_f = \frac{1}{\pi}\left[\frac{K_{Ic}}{F\sigma_{max}}\right]^2 \tag{4}$$

where K_{Ic} is the plane strain fracture toughness of the material. If the stress range and the initial and final flaw lengths are known, the total number of cycles to failure for a restored tooth with sub-surface flaws may be determined. An application of the Paris law to dental restorations requires that the opening mode global stress (σ) resulting from occlusal loading can be determined, and that the appropriate Paris law constants are available.

2.2. Finite element analysis

A finite element model (FEM) for a restored mandibular molar with Class II amalgam preparation was developed in this study to determine the stress distribution resulting from occlusal loading. A cross-section of the clinical crown was utilized for the proposed analysis, as shown in Fig. 1. Both the dimensions and shape of the molar were obtained from the permanent dentition traits reported by Kraus *et al.* [15]. A plane strain analysis was considered most appropriate according to the restoration configuration and displacement restriction promoted by adjacent teeth. Also, the maximum degree of deformation during mastication occurs primarily in the buccal and lingual directions due to the cusp geometry; elastic deformation in the distal direction is far smaller in comparison. Therefore, a plane strain analysis of the tooth is most consistent with the physiological conditions present in natural dentition.

Two different amalgam configurations were chosen to broaden the scope of the finite element analysis including a symmetric and non-symmetric geometry. The size and shape of the two amalgams examined in this study are shown in Fig. 2. A commercial computer-aided design and finite element software was used to develop the model geometry and finite element mesh for each restoration configuration [16]. Both the tooth and amalgam were meshed with four node plane strain isoparametric elements using an average element edge length of 0.25 mm. The symmetric and non-symmetric models were comprised of approximately 2200 and 1220 total elements, respectively.

Mechanical properties for the finite element model

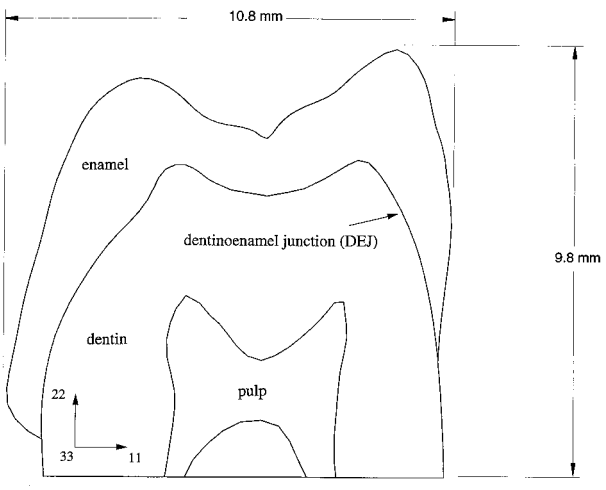

Figure 1 Unrestored crown model with dimensions.

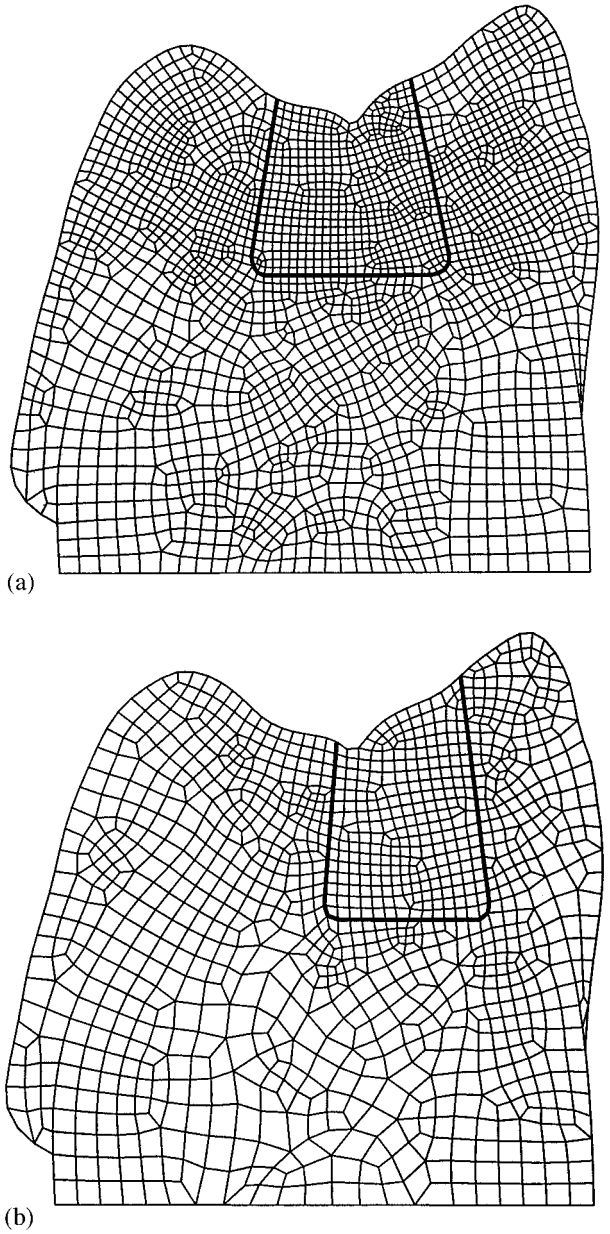

Figure 2 Schematic diagrams of the meshed models: (a) symmetric; (b) unsymmetric.

were obtained from a variety of sources. Properties of the dentine, pulp, and amalgam were obtained from a survey of the results reported and used by various investigators [17–20]. Each of these materials were assumed to exhibit isotropic behavior as reported. In contrast, the enamel was considered as an anisotropic material according to the recent work by Spears *et al*. [21]. Because the minor Poisson's ratio for enamel was not available, the reciprocal relation [22] was employed using the major and minor elastic moduli, and major Poisson's ratio available in the literature. All mechanical properties used for the finite element models are listed in Table I.

TABLE I Mechanical properties used in the finite element analysis

Material	E_1 (MPa)	E_2, E_3 (MPa)	v_{12}	v_{13}, v_{23}
Amalgam	50.0×10^3	50.0×10^3	0.29	0.29
Dentine	20.0×10^3	20.0×10^3	0.31	0.31
Enamel	80.0×10^3	20.0×10^3	0.30	0.08
Pulp	2.07	2.07	0.45	0.45

Following development of the solid models and finite element mesh, each model was processed using ABAQUS [23], another commercial finite element software, which permits an advanced treatment of contacting interfaces. Though limited information is available on the properties of the cavo-surface margin, it is generally accepted that the amalgam is not perfectly bonded. Therefore, the ability to model variations in the cavo-surface margin adhesion was an important necessity for this study. The pulpal floor was considered to be perfectly bonded under all conditions of analysis. However, the buccal and lingual margins were examined using conditions which describe both perfect and imperfect bonding. Perfect bonding required that both the tensile and compressive stresses remained continuous across the interface, whereas imperfect bonding conditions maintained only compressive stress continuity. Coloumb friction was also introduced along the cavo-surface margin to distinguish the relative contribution of mechanical interlocking along the interface; friction coefficients ranging from 0.0 to 4.0 were considered. The degree of mechanical interlocking could be a product of the surface texture resulting from cavity preparation or specific surface conditioning.

The boundary conditions for each model were specified through displacement restrictions at the base of the crown. Vertical and horizontal displacements at the base were assumed to be fixed according to the support provided by the alveolar socket. A distributed load was applied along the occlusal surface to simulate loads incurred during mastication. The distribution in occlusal load was achieved by applying the total load uniformly over 10 surface nodes beginning from the center and extending in the lingual direction as shown in Fig. 3. A cursory examination revealed that differences in the stress distribution resulting between a uniform and Gaussian load distribution were insignificant. Based on an average elemental length of approximately 250 μm, the total load was distributed across 2.5 mm of the occlusal surface. The total resultant force was varied from 0 to 300 N as per reports of occlusion by Bates *et al*. [24], and Carlsson [25]. In addition, the resultant load was adjusted between simulations from a vertical

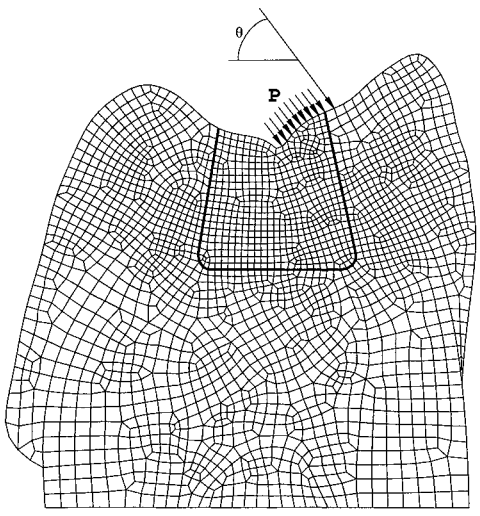

Figure 3 Tooth with boundary conditions and applied occlusal load (symmetric amalgam).

TABLE II The range in oral parameters included in the finite element analysis

Parameter	Range
Occlusal load	$P = 0$–$300\,N$
Occlusal load orientation	$\theta = 45°, 60°, 75°, 90°$
Cavo-surface bonding[a]	Perfect bonding and unbonded
Cavo-surface friction[b]	$\mu = 0.0, 1.0, 2.0, 3.0, 4.0$

[a]The pulpal floor is perfectly bonded in all simulations.
[b]Cavo-surface friction is not present during perfect bonding.

orientation (90°) to an orientation of 45°, in increments of 15°. Variations in the occlusal load orientation represent effects related to variations in occlusion and jaw symmetry. A summary of the range in oral conditions considered in the numerical analysis is highlighted in Table II.

3. Results

A finite element analysis of a mandibular molar with two different Class II amalgam restorations was conducted according to a specific set of analysis conditions as described in Table II. For each finite element simulation, the magnitude and location of maximum tensile stress within the molar were recorded. Although stresses within the amalgam were also examined, they were found to be consistently lower than those within the restored molar. At the location of either maximum normal or shear stress, the maximum principal stress and its orientation were determined. The normal $(\sigma_{11}, \sigma_{22})$ and shear stress (σ_{12}) distribution within the unsymmetric amalgam restoration which results from mastication is shown in Fig. 4; a 200 N occlusal load with 60° orientation and coefficient of friction equal to 4.0 were used for the simulation. The stress contours in this figure clearly elucidate the geometric stress concentration resulting near the pulpal floor. Regardless of occlusal load or marginal friction, the maximum principal stress in each restored molar was found to exist within the dentine near the pulpal floor and cavo-surface margin junction. Furthermore, through a comparison of the stress distribution from various simulations, the influence of occlusal load and cavo-surface margin adhesion were clearly apparent.

3.1. Occlusal load

Variations in the occlusal load orientation and magnitude had significant effects on the stress distribution within both restored molars, as expected. An increase in the horizontal component of loading with change in occlusal load orientation from 90° to 45° resulted in an increase in the tensile stress distribution. Also, the stress distribution increased linearly with increasing applied load according to the linear elastic material response. Based on the linear distribution between the occlusal load and resulting stress distribution, a mathematical relationship for the maximum principal stress (σ_1) in terms of the applied load was determined for each load orientation $(\sigma_1(P)|_\theta)$. The maximum principal stress that developed within each restored molar over the range in occlusal loads and orientations is shown in Fig. 5; the stresses reported in this figure result from an interfacial friction coefficient along the cavo-surface margin of 0.0. Note that the stress resulting from any applied load can be distinguished from this figure using either an interpolation or extrapolation as needed.

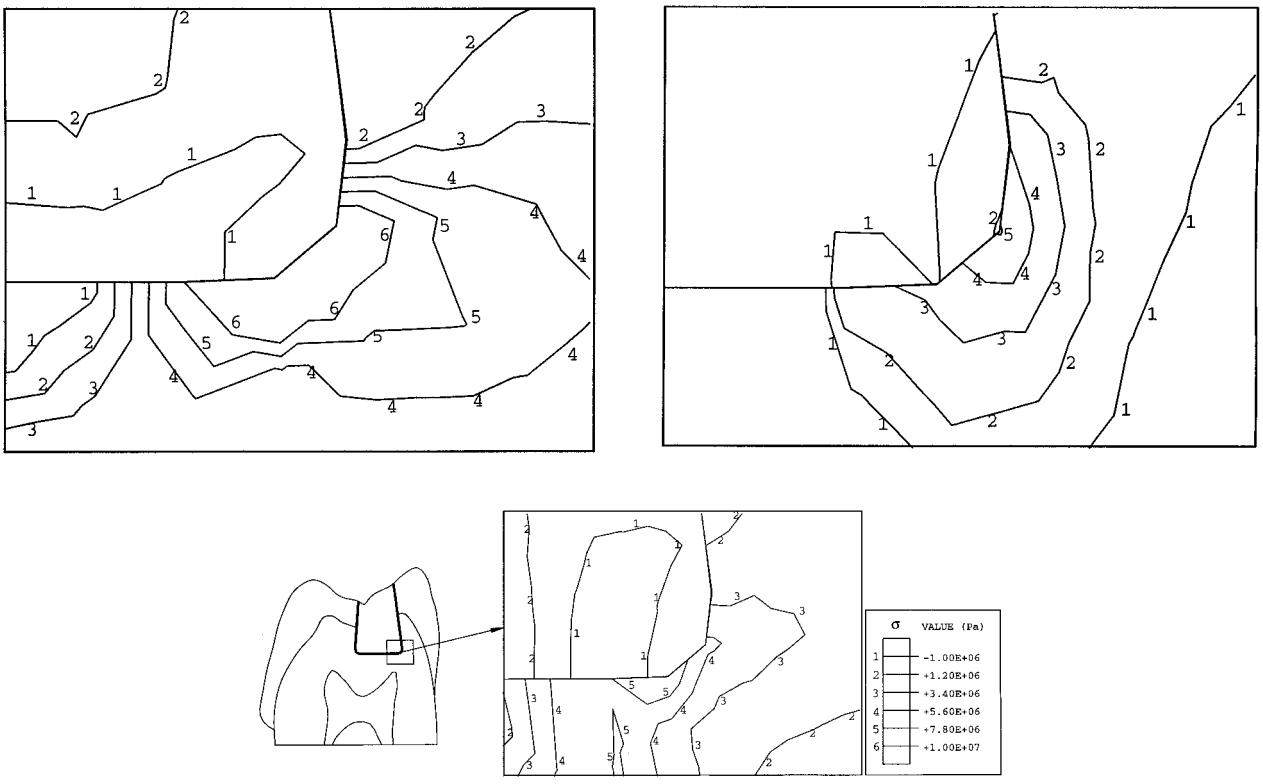

Figure 4 The stress distribution within the molar restored with an unsymmetric amalgam (load = 200 N, $\theta = 60°$, $\mu = 4.0$). The stress contours are provided for the highlighted region: (a) σ_{11}; (b) σ_{22}; (c) σ_{12}.

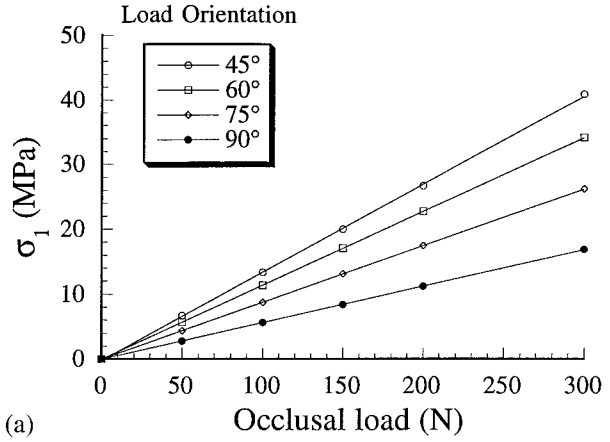

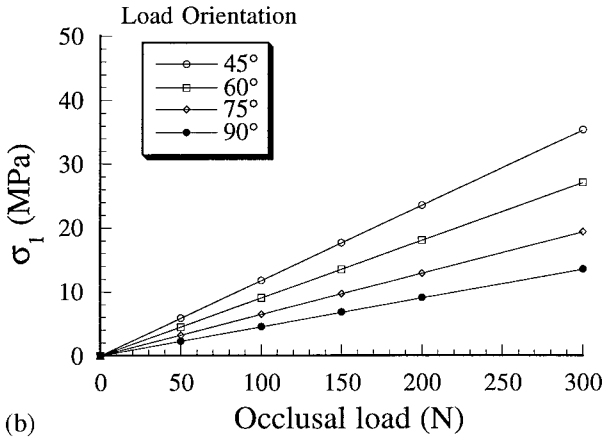

Figure 5 The influence of occlusal load orientation on the magnitude of maximum principal stress ($\mu = 0.0$): (a) symmetric amalgam; (b) unsymmetric amalgam.

In addition to examining the in-plane stress distribution (σ_{11}, σ_{22} and σ_{12}), the out of plane stress (σ_{33}) resulting from occlusal loading was also recorded. Due to the nature of in-plane tensile stresses near the cavity floor, as shown in Fig. 4, the out-of plane stress that developed in the distal direction was also tensile in nature. Note that according to the plane strain assumption, σ_{33} is actually the intermediate principal stress (σ_2) following the convention $\sigma_1 \geq \sigma_2 \geq \sigma_3$. Consequently, the out of plane stress increased with an increase in horizontal occlusal loading as well.

3.2. Cavo-surface bonding

The effects of cavo-surface margin adhesion on the stress distribution which results from occlusal loading were readily apparent. Perfect bonding on the buccal and lingual margins (resulting in perfect bonding over the entire amalgam surface) promoted tensile stresses which were significantly lower than those present for debonded interfaces. Peters and Poort [26] reported similar results while examining the stress distribution of a restored mandibular molar under occlusal loading using an axisymmetric finite element model. The reduction in stress with cavo-surface adhesion results primarily from a decrease of the in-plane normal stress (σ_{22}) and shear stress (σ_{12}). A comparison of the stress distribution within each restored molar which results from perfect bonding and no bonding is shown in Fig. 6; an occlusal load of 200 N with 60° orientation has been applied to each restored tooth in this simulation. Results for the perfectly bonded and partially debonded interfaces of the symmetric restoration are shown in Fig. 6a and b, respectively; the corresponding stress distribution for the unsymmetric amalgam is shown in Fig. 6c and d. Note that the pulpal floor was considered to be perfectly bonded for both models. Loss of adhesion along the cavo-surface margin results in a concentration of compressive normal stress (σ_{22}) within the amalgam. Compressive stresses focused in the amalgam augment Poisson's expansion and consequently result in an increase in bending stresses and shear stress within the supporting dentinal ligament.

3.3. Cavo-surface margin friction

Marginal friction is a product of surface roughness and the degree of interdigitated amalgam which results from the methods used for cavity preparation. In comparison to the influence of load orientation and interfacial bonding, friction along the cavo-surface margin was found to be far less important. Nevertheless, the maximum principal stress (σ_1) within both restored molars decreased with increasing coefficient of friction (μ), as clearly apparent in Fig. 7. The stress distribution in these figures resulted from an occlusal load of 200 N at an orientation of 75° from the horizontal plane. As the orientation of occlusal loading approached 90°, the influence of interfacial friction decreased. From a comparison of results from the two amalgam configurations in Fig. 7, friction had slightly more influence on the molar restored with an unsymmetric amalgam.

Although cavo-surface friction had minimal influence on the magnitude of principal stress, it played a much larger role on the principal stress orientation. Changes in the principal axis orientation with μ were attributed to changes in the in-plane shear (σ_{12}) and transverse normal stress (σ_{11}). Consequently, the extent of crack propagation required to reach the critical flaw length (a_f) according to Equation 4 changes because of the change in orientation of the maximum opening mode stress. The most significant influence of cavo-surface friction occurred from masticatory loads with substantial horizontal components of occlusal loading ($\theta = 45°$).

4. Discussion

A finite element analysis of the stress distribution within two restored mandibular molars with different standard Class II amalgam restorations was conducted. The magnitude and location of maximum principal stress was distinguished as a function of the oral conditions and masticatory load. Regardless of occlusal load or cavo-surface margin adhesion, it was found that the largest maximum principal stress resulted within the dentine, near the juncture of the buccal plane and pulpal floor. Therefore, if subsurface cracks were introduced to the molar during cavity preparation, the fatigue crack growth rate resulting from mastication would be greatest at this location. The aforementioned statement is based on the assumption that the fracture toughness of dentine is

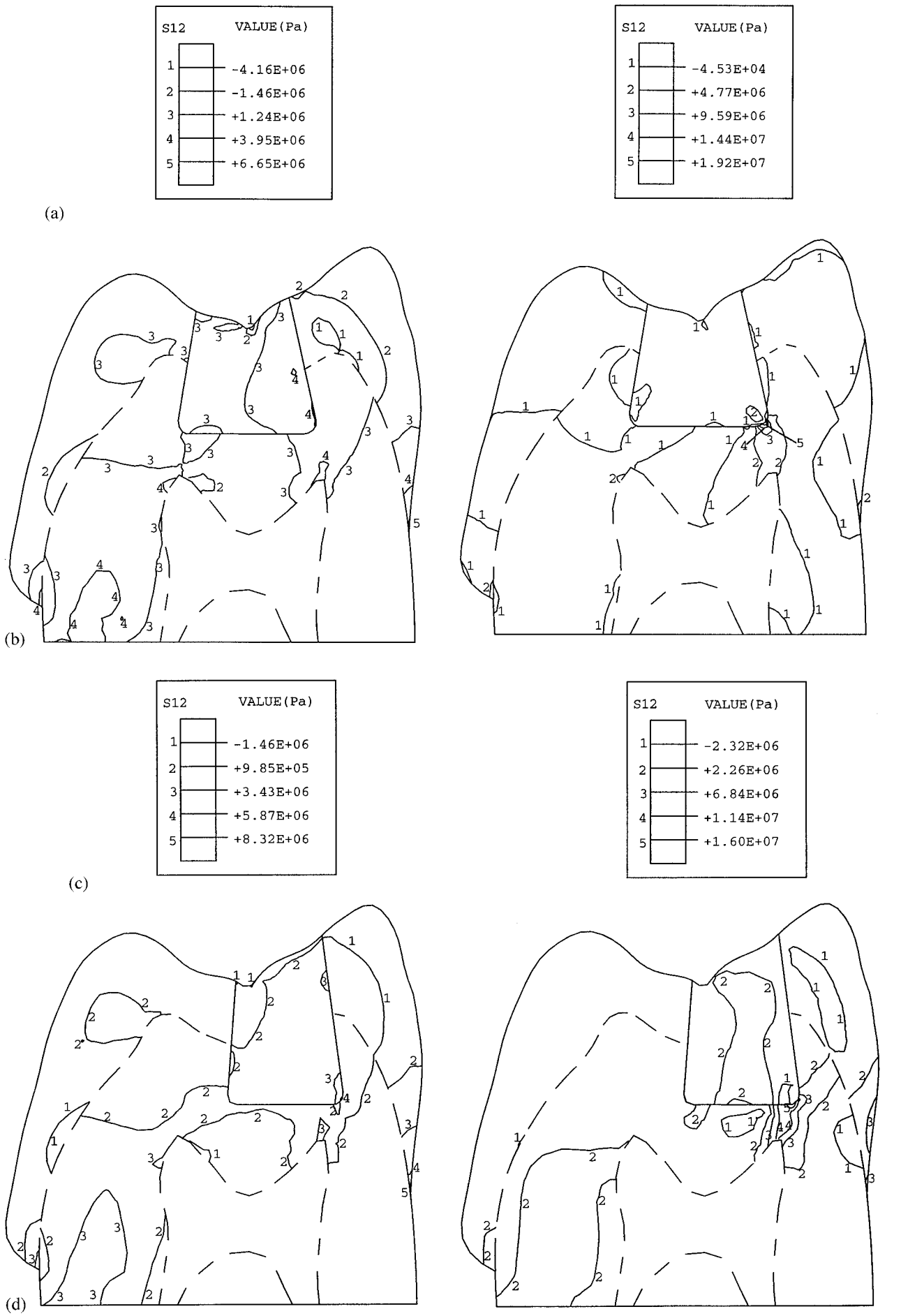

Figure 6 A comparison of the stress distribution resulting from cavo-surface bonding (load = 200 N, $\theta = 60°$): (a) symmetric (tied); (b) symmetric (untied); (c) unsymmetric (tied); (d) unsymmetric (untied).

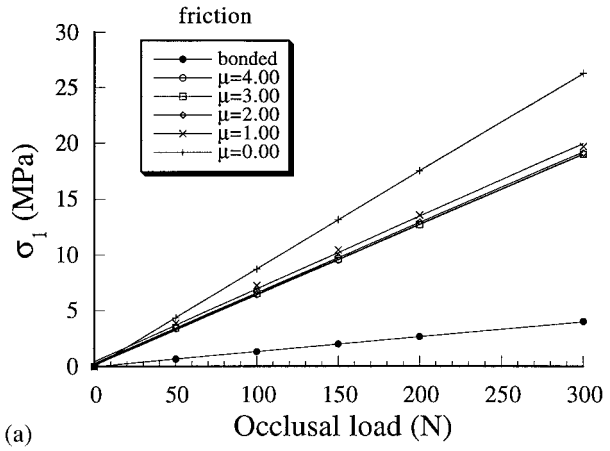

(a)

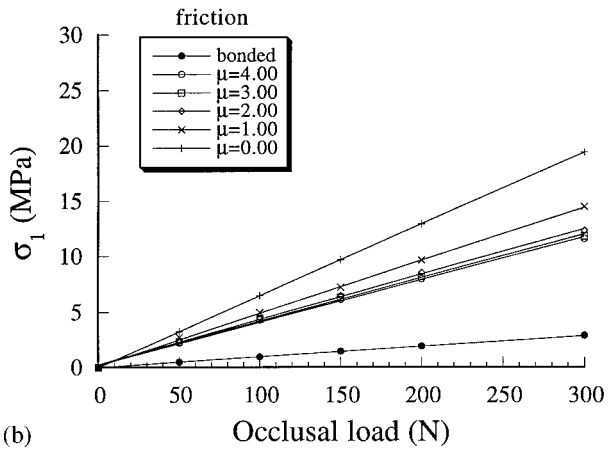

(b)

Figure 7 The influence of friction along the cavo-surface margin on the magnitude of maximum principal stress ($\theta = 75°$): (a) symmetric amalgam; (b) unsymmetric amalgam.

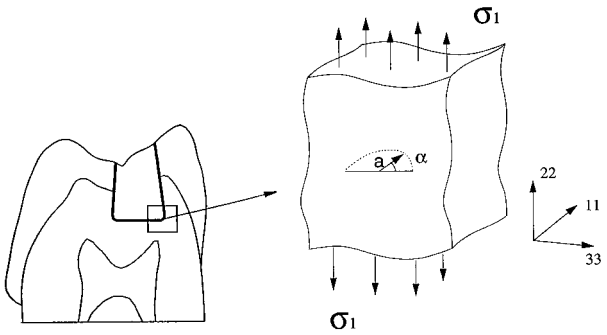

Figure 8 Location and geometry of the subsurface crack resulting from cavity preparation.

independent of location (or relative distance from the dentinoenamel junction).

According to Equations 2 and 3, a prediction of the fatigue life for a restored tooth requires that the global cyclic stress range ($\Delta\sigma$) is known. Results from the finite element analysis provided the maximum stress ($\sigma_{max} = \sigma_1$) resulting from mastication and its location within both restored molar configurations. The minimum stress (σ_{min}) occurs every masticatory cycle and is equal to zero. Therefore, the stress range from mastication is mathematically equal to the magnitude of maximum principal stress ($\Delta\sigma = \sigma_1$). Fatigue crack growth may also occur due to the out of plane stress ($\sigma_{33} = \sigma_2$). Nevertheless, the in-plane stress intensity range computed according to Equation 2 is greatest because of the magnitude of in-plane stress. In addition to the stress range, a fatigue life prediction requires knowledge of the initial and final crack lengths, and the geometry factor (F). As previously discussed, Xu *et al.* [13] quantified subsurface cracks in enamel which was prepared with diamond burs. Using an optical analysis, flaws were found below the machined surface that extended to depths of $80 \pm 34\,\mu m$. Subsurface flaw lengths resulting from clinical preparation of dentine with dental instruments have not been reported. According to measurements of subsurface flaws resulting from cavity preparation in enamel, initial flaw lengths that range between 20 and 150 μm were considered to be most appropriate for the present study.

The geometry factor (F) which accounts for the specific crack and specimen geometry may be obtained from handbooks. Xu *et al.* [13] found that cracks resulting from cavity preparation typically existed perpendicular to the surface as a median crack. Assuming that the cracks can be adequately defined as a penny-shaped surface crack in a semi-infinite medium as shown in Fig. 8, the geometry factor is given by [29]

$$F = \frac{2}{\pi}\{1.04[1 + 0.1(1 - \sin\alpha)^2]\} \qquad (5)$$

where α is the angle from the cavo-surface margin to the point of interest. Utilizing the average F over the range in α, and the maximum stress range for both molar configurations in Fig. 5 ($\Delta\sigma = 35$ MPa), the stress intensity range (ΔK) was calculated according to Equation 2. The maximum ΔK for the two restored molars with subsurface cracks located along the cavo-surface margin is $0.52\,MPa\,m^{1/2}$.

The final or critical flaw length (a_f) in which gross fracture of the tooth encasement occurs must also be found to predict the restoration fatigue life. For a subsurface crack located within the dentine, as shown in Fig. 8, the critical flaw length may be found using the maximum applied stress and fracture toughness of dentine as noted from Equation 4. The fracture toughness (K_{Ic}) of human enamel and dentine have been reported under both standard laboratory conditions [27] and aqueous environments [28]. An average value for the fracture toughness of dentine from these reports was found equal to $3.0\,Mpa\,m^{1/2}$. Using this quantity, the critical flaw length (a_f) estimated as outlined in Equation 4 exceeds the distance from the cavo-surface margin to the lingual surface (approximately 3 mm). Note that the final flaw length is influenced by the oral conditions (margin adhesion and interfacial friction) and occlusal load due to their influence on the maximum principal stress. The maximum stress which causes tooth fracture is not necessarily the maximum cyclic stress distinguished from the finite element analysis. Tooth fracture is typically associated with the application of occlusal loads which are much greater in magnitude than those which occur during routine mastication. An increase in the occlusal load or reduction in fracture toughness (associated with crack propagation into the enamel) reduces the critical crack length necessary for fracture to

occur. According to Equation 4, the crack reaches a crtical length immediately upon reaching the dentino-enamel junction due to the extremely low fracture toughness of enamel. Hence, a_f is the distance from the crack tip to the dentino-enamel junction with an orientation which is defined by the plane of maximum opening mode stress (σ_1). Based on these considerations, a critical flaw length of 2.5 mm is chosen as an appropriate final flaw length which facilitates gross tooth fracture according to LEFM.

The Paris law parameters for dental biomaterials including C and m in Equation 1 have not been reported in the open literature. These properties are required for a meaningful estimate of the cyclic fatigue life for restored teeth. From inspection, the mechanical properties of teeth and engineering ceramics are quite similar. In fact, the fracture toughness and hardness of aluminum oxide (Al_2O_3) are well within that reported for dentine and enamel. Therefore, the Paris law constants for Al_2O_3 are used in this investigation to conduct a cursory fatigue life estimate of the molars with amalgam restorations. Suresh [14] has reported the Paris law coefficient and exponent (C and m) for Al_2O_3 from a survey of experimental studies. The parameters obtained from studies with similar load ratios $(R = (\sigma_{min}/\sigma_{max}) \cong 0)$ are listed in Table III.

Utilizing the maximum tensile stresses determined from the finite element simulations reported in Fig. 5, and appropriate material properties as previously described, the range in cyclic fatigue life for the restored molars was estimated in terms of an assumed initial subsurface crack length. The resulting fatigue life estimates are shown in Fig. 9. As the appropriate fatigue properties for the dental biomaterials were unavailable, the fatigue life is plotted over the range in Paris law parameters for Al_2O_3 listed in Table III. Variations in life with the Paris law exponent, and coefficient are plotted in Fig. 9a and b, respectively. Note that the parameter space which results in a restoration life of less than 25 years is highlighted. As evident in both figures, the initial subsurface crack length resulting from cavity preparation has a significant effect on the restoration life. In fact, flaws initiated within the dentine equivalent in length to those observed by Xu *et al.* [13] in enamel may result in a fatigue life well below 25 years. Cracks larger than 100 μm could result in a fatigue life of less than 5 years. The range in fatigue life distribution in Fig. 9a suggests that flaws as small as 25 μm could promote restoration failure well within 25 years. Therefore, the introduction of subsurface flaws during cavity preparation could be the principal source for tooth fracture and a major obstacle for lifelong oral health. No study has previously identified the significance of subsurface cracks initiated during cavity preparation on the failure of dental restorations.

Sakaguchi *et al.* [30] also used the Paris law in estimating fatigue crack growth rates in full crown restorations. Similar to limitations faced in the present study, Paris law parameters for the restorative dental materials were not available. Perhaps more important than the Paris law parameters is the fatigue threshold (ΔK_{th}); ΔK_{th} is the threshold stress intensity below which the fatigue crack growth rate of long cracks is insignificant. The maximum stress intensity range for the molars in this study was found to be approximately 0.5 MPa $m^{1/2}$. However, ΔK_{th} for dental biomaterials has not been reported. Interestingly, it has recently been found that the fatigue crack growth rates of short fatigue cracks with small ΔK are significantly greater than that for long cracks. The subsurface crack lengths expected to exist within either enamel or dentine along the cavo-surface margin would be classified as short fatigue cracks. Therefore, the detrimental effects of subsurface flaws introduced during cavity preparation could be much more significant than predicted in this study. Hence, the fatigue crack growth parameters, including the fatigue threshold, must be determined through further investigation to distinguish the contribution of sub-surface flaws to the success of dental restorations.

5. Conclusions

A finite element analysis of a mandibular molar restored with two different Class II amalgam preparations was conducted. The stress distribution which results from occlusal loading within each restored molar was found in terms of the occlusal load and specific interfacial conditions along the cavo-surface margin. Using the stress distribution resulting from mastication, a fatigue life analysis of the restored tooth was conducted using the Paris law for cyclic fatigue crack growth. Subsurface cracks were assumed to exist along the restoration boundary resulting from cavity preparation. Based on the results obtained from this analysis, the following conclusions are made:

1. A finite element analysis of the restored mandibular molar with different Class II preparations showed that the maximum tensile stress in the tooth occurred within the dentine at the juncture of the lingual margin and pulpal floor. The largest tensile stress occurred in the tooth restored with a symmetric amalgam. Tensile stresses were found to develop within the dentine regardless of the orientation of occlusal loading or degree of adhesion between the amalgam and cavity.

TABLE III The range in Paris law parameters reported for aluminum oxide from experimental studies with low stress ratio (R) [14]

Material	Stress ratio	C, m/cycle $(MPa\,m^{1/2})^{-m}$	m	ΔK $(MPa\,m^{1/2})$
Al_2O_3 (90% pure)	$R = 0.15$	2.8×10^{-10}	10	1.0–3.0
	$R = 0.15$	6.3×10^{-11}	8	2.0–3.5
Al_2O_3 (33 vol% SiC whiskers)	$R = 0.15$	4.5×10^{-10}	7	3.5–6.0
	$R = 0.15$	4.0×10^{-10}	4	3.5–6.0

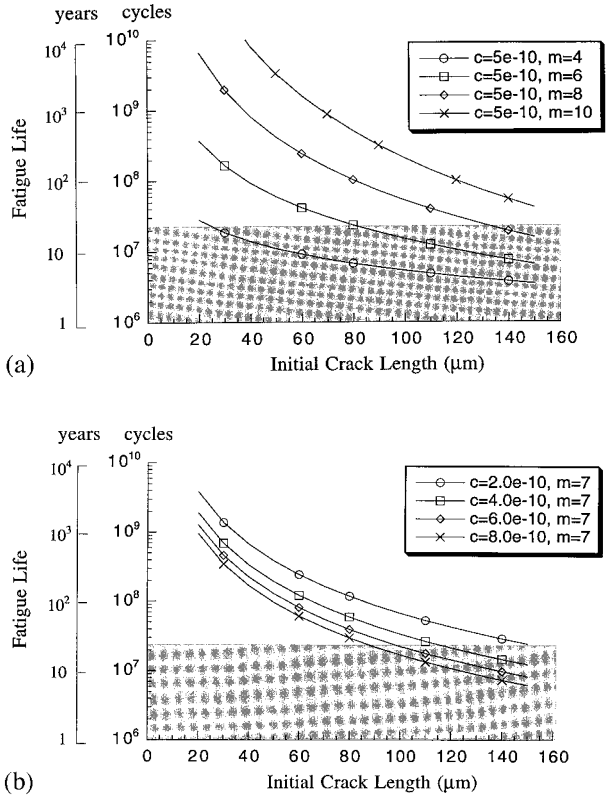

Figure 9 The influence of subsurface flaw length along the cavo-surface margin on the fatigue life of molars with a standard amalgam preparation. Life is predicted according to the Paris law ($da/dN = C\Delta K^m$) under zero to tension loading ($R = 0$). The highlighted area represents the parameter space which promotes a restoration life less than 25 years: (a) variation in life with m; (b) variation in life with C.

2. The contribution of friction along the cavo-surface margin had minimal influence on the location of the maximum principal stress. The maximum tensile stress was found to increase with decreasing friction coefficient (μ) which results from the lack of marginal bonding and/or tabbing. In contrast to the characteristics of an imperfect margin, adhesion along the lingual and buccal planes significantly reduced the maximum tensile stresses that develop during mastication.

3. The propensity for cyclic fatigue crack growth in restored molars was examined using the Paris law. Because of the absence of reports on the fatigue properties for dental materials, the Paris law parameters reported for aluminum oxide were used for a preliminary analysis. It was found that cyclic fatigue crack growth in restored teeth may contribute significantly to premature restoration failure. The fatigue life of restored molars predicted using the Paris law was as low as 5 years. Therefore, the instruments and techniques currently used in cavity preparation should be examined more closely. The development of subsurface cracks during cavity preparation should now be considered as a principal source for premature restoration failure.

4. A comprehensive prediction for the fatigue life of dental restorations requires a determination of the fatigue properties for biological dental materials. The appropriate parameters necessary for predicting the fatigue life of dental materials are currently not available. Therefore, future research must be focused on determining the fatigue properties of teeth and investigations which further define the role of subsurface flaws on the fatigue life of restored teeth.

Acknowledgment

The authors graciously acknowledge financial support through a Designated Research Initiation Fund, No. 05388602. The authors would also like to thank Mr Kirk Stoffel, an undergraduate student at UMBC, for assistance with the finite element simulations.

References

1. D. L. MOORE and J. L. STEWART, *J. Prosth. Dent.* **17** (1967) 372.
2. J. GOLDBERG, J. TANZER and E. MUNSTER, *J. Amer. Dent. Ass.* **102** (1981) 635.
3. B. A. WHITE, T. F. ALBERTINI, L. J. BROWN, D. LARACH-ROBINSON, M. REDFORD and R. H. SELWITZ, *J. Dent. Res.* **75** (1996) 661.
4. R. L. LAMBERT, in ''Amalgam restorations in advanced restorative dentistry,'' edited by L. Baum (W. B. Saunders Co., Philadelphia, 1973).
5. W. A. VALE, *Irish Dent. Rev.* **2** (1956) 33.
6. G. J. RE and B. K. NORLING, *J. Dent. Res.* **60** (1981) 805.
7. N. D. RUSE, PhD Dissertation, University of Toronto, 1988.
8. L. E. TAM and R. M. PILLIAR, *J. Dent. Res.* **72** (1993) 953.
9. T. F. WATSON, *ibid.* **70** (1991) 44.
10. *Idem., J. Microsc.* **157** (1990) 51.
11. *Idem., J. Dent. Res.* **69** (1990) 1531.
12. T. F. WATSON and A. BOYDE, *ibid.* **68** (1989) 577.
13. H. H. K. XU, J. R. KELLY, S. JAHANMIR, V. P. THOMPSON and E. D. REKOW, *ibid.* 1997, in press.
14. S. SURESH, in ''Fatigue of materials,'' (Cambridge University Press, Cambridge, 1991).
15. B. S. KRAUS, R. E. JORDAN and L. ABRAMS, in ''A study of the masticatory system: Dental anatomy and occlusion,'' (Williams and Wilkins Company, Baltimore, MD, 1969).
16. IDEAS, Structural Dynamics Research Corporation, Masters Series 5.0, (Milford OH, 1990).
17. R. G. CRAIG and F. A. PEYTON, *J. Dent. Res.* **40** (1961) 936.
18. B. VAN MEERBEEK, G. WILLEMS, J. P. CELIS, J. R. ROOS, M. BRAEM, P. LMBRECHTS and G. VANHERLE, *ibid.* **72** (1993) 1434.
19. R. W. THRESHER and G. E. SAITO, *J. Biomech.* **6** (1973) 443.
20. W. J. O'BRIEN, in ''Dental materials and their selection,'' 2nd edition (Quintessence Publishing Co., Illinois, 1997).
21. I. R. SPEARS, R. VAN NOORT, R. H. CROMPTON, G. E. CARDEW and I. C. HOWARD, *J. Dent. Res.* **72** (1993) 1526.
22. R. M. JONES, in ''Mechanics of composite materials,'' (Hemisphere Publishing Corp., 1975).
23. K. A. S. ABAQUS, Hibbit Inc., Version 5.7, (Providence RI, 1998).
24. J. F. BATES, G. D. STAFFORD and A. HARRISON, *J. Oral Rehab.* **2** (1975) 349.
25. G. E. CARLSSON, *Front. Oral Phys.* **1** (1974) 265.
26. M. C. R. B. PETERS and H. W. POORT, *J. Dent. Res.* **62** (1983) 358.
27. O. M. EL MOWAFY and D. C. WATTS, *ibid.* **65** (1986) 677.
28. S. T. RASMUSSEN and R. E. PATCHIN, *ibid.* **63** (1984) 1362.
29. J. C. NEWMAN and I. S. RAJU, in ''Computational methods in the mechanics of fracture,'' edited by S. N. Atluri (Elsevier North Holland, New York, 1986).
30. R. I. SAKAGUCHI, M. CROSS and W. H. DOUGLAS, *Dent. Mater.* **8** (1992) 131.

Received 1 September
and accepted 21 September 1998